



City Research Online

City, University of London Institutional Repository

Citation: De Martino, A., Dell'Anna, L. & Egger, R. (2007). Magnetic barriers and confinement of Dirac-Weyl quasiparticles in graphene. *Solid State Communications*, 144(12), pp. 547-550. doi: 10.1016/j.ssc.2007.03.062

This is the accepted version of the paper.

This version of the publication may differ from the final published version.

Permanent repository link: <https://openaccess.city.ac.uk/id/eprint/14088/>

Link to published version: <https://doi.org/10.1016/j.ssc.2007.03.062>

Copyright: City Research Online aims to make research outputs of City, University of London available to a wider audience. Copyright and Moral Rights remain with the author(s) and/or copyright holders. URLs from City Research Online may be freely distributed and linked to.

Reuse: Copies of full items can be used for personal research or study, educational, or not-for-profit purposes without prior permission or charge. Provided that the authors, title and full bibliographic details are credited, a hyperlink and/or URL is given for the original metadata page and the content is not changed in any way.

City Research Online:

<http://openaccess.city.ac.uk/>

publications@city.ac.uk

Magnetic barriers and confinement of Dirac quasiparticles in graphene

A. De Martino* L. Dell'Anna R. Egger

Institut für Theoretische Physik, Heinrich-Heine-Universität, D-40225 Düsseldorf, Germany

Abstract

We discuss the properties of the two-dimensional massless Dirac quasiparticles emerging as low-energy charge carriers in graphene, in the presence of inhomogeneous magnetic fields. We show that, in contrast to electrostatic fields, appropriate configurations of magnetic field can confine the quasiparticles. Our results open up the way to the possibility of designing mesoscopic structures in graphene, as e.g. quantum dots, by means of magnetic barriers.

Key words: graphene, inhomogeneous magnetic field, quantum dot

PACS: 73.21.-b, 75.70.Ak

1 Introduction

Recently, the existence of stable two-dimensional (2D) monolayers of graphite, also known as graphene, has been experimentally demonstrated [1–3]. This discovery sparked an intense experimental and theoretical activity, both on fundamental aspects of quantum transport in graphene, as well as on its possible applications as building block of future nanoelectronic devices.

The peculiarity of graphene stems from the fact that its Fermi surface reduces to two points, the inequivalent vertices of the hexagonal Brillouin zone of graphene's honeycomb lattice, conventionally called K and K'. In proximity of each of these Fermi points the spectrum has the shape of a double cone, which

* Corresponding author: A. De Martino

Email addresses: ademarti@thphy.uni-duesseldorf.de (A. De Martino),
luca@thphy.uni-duesseldorf.de (L. Dell'Anna),
egger@thphy.uni-duesseldorf.de (R. Egger).

is a typical relativistic massless spectrum. Together with the lattice structure, this results into low-energy quasiparticles which behave as chiral Dirac-Weyl (DW) particles of zero mass, whereby the two sublattices of graphene's honeycomb lattice lead to the (iso-)spin degree of freedom. This unique electronic dispersion has been by now verified experimentally [1–4].

It is well known that electrostatic barriers are unable to confine DW particles due to the phenomenon of Klein tunneling [5,6]. Essentially, under an electrostatic barrier, the Dirac sea is shifted upwards, and incident quasiparticles can propagate via empty quasihole states, and eventually be perfectly transmitted. In graphene this phenomenon makes problematic the design of electronic devices, where quasiparticles are typically confined by means of electrostatic fields.

To overcome this problem, we noticed that, in contrast to electrostatic fields, it is possible to confine graphene's Dirac quasiparticles by means of *magnetic barriers* [7]. In essence, this possibility stems from the fact that, irrespectively of the quasiparticles relativistic nature, magnetic fields deflect their trajectories via the Lorentz force. One can then, by appropriate engineering, create a *inhomogeneous* field configuration which traps the quasiparticles in a restricted region. Existing technology, already employed to create and investigate confining inhomogeneous field configurations for two-dimensional electron gases in conventional semiconductor heterostructures, could be used for the same purpose in graphene.

To illustrate this idea, let us consider a graphene layer (located in the $(x - y)$ plane) in a perpendicular magnetic field $\mathbf{B} = B(x, y)\hat{e}_z$. We only consider the orbital effect, but the inclusion of a Zeeman term is straightforward and does not affect our conclusions. Accordingly, the spin index will be henceforth omitted. The length scale λ_s over which \mathbf{B} varies significantly is assumed to be much larger than graphene's lattice spacing ($a = 0.246$ nm). At low-energy the graphene layer is then described by two copies of the Dirac-Weyl Hamiltonian, which are interchanged by the time reversal operation. Each copy describes the electronic states close to the relevant K point. Under the condition $\lambda_s \gg a$ the magnetic field cannot scatter quasiparticles from one K-point to the other [8], and one can focus on a single K point. The time-independent Weyl equation for the spinor $\psi(x, y) = (\psi_+, \psi_-)^T$ at energy $E = v_F \epsilon$ and magnetic field $\mathbf{B} = \text{rot}\mathbf{A}$ then reads (we set $\hbar = 1$)

$$\left(\mathbf{p} + \frac{e}{c} \mathbf{A}(x, y) \right) \cdot \vec{\sigma} \psi(x, y) = \epsilon \psi(x, y), \quad (1)$$

where $v_F \approx 8 \times 10^5$ m/sec is the Fermi velocity, $\mathbf{p} = -i(\partial_x, \partial_y)^T$ the momentum operator, and the 2×2 Pauli matrices $\vec{\sigma} = (\sigma_x, \sigma_y)^T$ act in isospin space. The two components of ψ describe the quasiparticle probability amplitudes on the

two sublattices of graphene's lattice. It is also convenient to introduce the gauge invariant velocity operator given by $\mathbf{v} = v_F \vec{\sigma}$.

2 Magnetic barrier

Let us consider first the case of a *magnetic barrier*, i.e. a field $B(x, y)$ uniform in the y -direction, and non-vanishing (and, say, positive) only in a finite region of size $2d$ around the origin in the x direction. We shall see that simple arguments predict that the magnetic barrier, in a certain range of quasiparticle energies, is *perfectly reflecting*. This has to be contrasted with the perfect transmission of quasiparticles through electrostatic barriers via Klein tunneling.

If the length scale λ_s is much smaller than the quasiparticle Fermi wave length λ_F , we can approximate $B(x, y)$ as a square barrier of width $2d$, $B(x, y) = B_0 \theta(d^2 - x^2)$, where $\theta(x)$ is the Heaviside step function. Since $\lambda_F \sim 1/|\epsilon|$, at low enough energy this approximation is always justified. Accordingly the vector potential can be chosen as $\mathbf{A}(x, y) = A(x) \hat{e}_y$, with $A(x)$ given by

$$A(x) = \frac{c}{el_B^2} \times \begin{cases} -d, & x < -d \\ x, & |x| \leq d \\ d, & x > d \end{cases}, \quad (2)$$

with the magnetic length $l_B \equiv \sqrt{c/eB_0}$. In this gauge, conservation of the momentum p_y parallel to the barrier allows us to reduce the two-dimensional problem to one-dimension, whereby Eq. (1) reduces to two decoupled one-dimensional Schrödinger equations

$$[\partial_x^2 - V_{\pm}(x) + \epsilon^2] \psi_{\pm}(x) = 0, \quad (3)$$

with p_y -dependent effective potentials $V_{\pm}(x) = \pm(e/c)\partial_x A(x) + [p_y + (e/c)A(x)]^2$ for the upper and lower components of the spinor ψ .

We now focus on the scattering problem defined by Eq. (3). We consider an electron-like scattering state of energy $\epsilon > 0$ incident from the left side of the barrier with velocity $\mathbf{v} = v_F(\cos \phi, \sin \phi)^T$ and momentum $\mathbf{p} = (p_x, p_y)$, with $|p_y| < \epsilon$. Momentum and velocity are related by

$$p_x = \epsilon \cos \phi, \quad p_y = \epsilon \sin \phi + d/l_B^2. \quad (4)$$

The incoming wave function is, up to an overall normalization,

$$\psi_{in}(x) = \begin{pmatrix} 1 \\ e^{i\phi} \end{pmatrix} e^{ip_x x}, \quad (5)$$

and the corresponding outgoing state is given by

$$\psi_{out}(x) \propto \begin{pmatrix} 1 \\ e^{i\phi'} \end{pmatrix} e^{ip'_x x}. \quad (6)$$

The emergence angle ϕ' , defined by $p'_x = \epsilon \cos \phi'$, is given by conservation of the longitudinal momentum p_y as

$$\sin \phi' = \frac{2d}{\epsilon l_B^2} + \sin \phi. \quad (7)$$

Eq. (7) shows that in a certain range of values of the incidence angle ϕ , the transmission probability vanishes. In fact, under the condition

$$\epsilon l_B \leq d/l_B, \quad (8)$$

we find *perfect reflection* for any incidence angle, as every incoming state of low enough energy is strongly deflected under the barrier and exits backwards. This illustrates our main finding: in contrast to electrostatic barriers, *magnetic barriers are able to confine Dirac-Weyl quasiparticles*. This analysis does not depend on the details of the magnetic field profile, and the conclusion is thus generic, provided the condition $a \ll \lambda_s \ll \lambda_F$ is satisfied.

For the approximate square-well magnetic profile, the scattering problem can be solved analytically, by matching the wave functions at the edges of the barrier. The details of the solution can be found in [7]. The resulting transmission probability $T(\epsilon, \phi)$ is plotted in Figure 1 as a function of the energy for two different values of the barrier width and several values of the angle ϕ . The figures illustrate the transmission profile with the perfect reflection regime which is entered at sufficiently low energy and/or large barrier. The magnetic length for a typical value of $B_0 = 6$ T is $l_B = 10$ nm, and $\epsilon l_B = 1$ corresponds then to $E = 50$ meV. Standard fabrication and doping techniques should thus be sufficient to reach the zero-transmission regime.

For negative values of the longitudinal momentum p_y the effective 1d Schrödinger potentials in the barrier region develop a minimum which lies below the value of the potential outside the barrier. In this situation there exist bound states

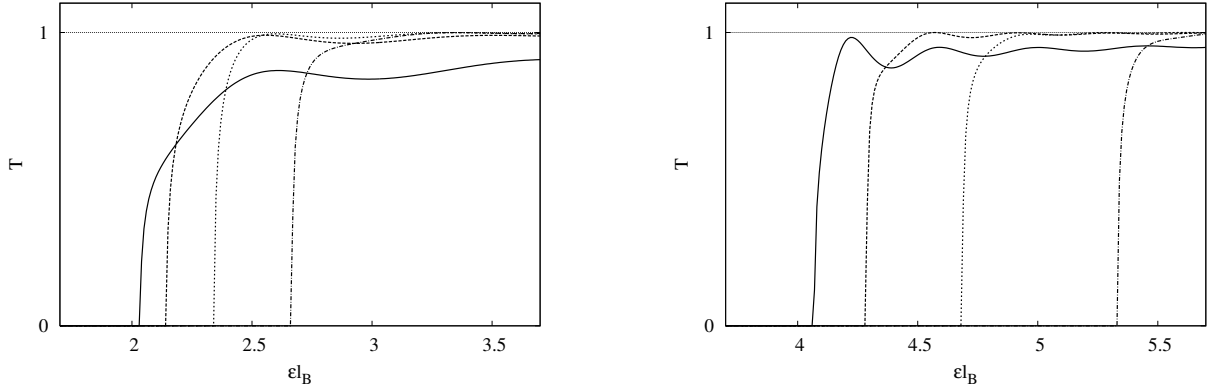


Fig. 1. Transmission probability for the magnetic barrier plotted as a function of the energy for two values of barrier width, $d = 2l_B$ and $d = 4l_B$. The different curves correspond, from right to left, to the angles $\phi = -n\pi/12$, with $n = 2, 3, 4, 5$.

solutions to Eq. (3), with energy $|\epsilon| < |p_y|$, which are localized at the edges of the barrier and describe quasiparticles trapped at the discontinuity of the magnetic field. They are analogous to the edge states which arise in conventional 2DEG with electrostatic confinement, and provide one-dimensional channels propagating along the barrier, which are crucial to the transport properties of the system. To describe more quantitatively these *magnetic edge states* we focus on a single edge of the barrier (say, the left one). Under the assumption that the edge smearing length $\lambda_s \ll \lambda_F$, the magnetic field profile can then taken as a step function $B(x, y) = B_0\theta(x)$, and correspondingly the vector potential can be taken as $A(x) = cx\theta(x)/el_B^2$. The spectrum of bound states is then given by the roots of the equation

$$\left(\sqrt{p_y^2 - \epsilon^2} - p_y\right) D_{(\epsilon l_B)^2/2-1}(\sqrt{2}p_y l_B) + \sqrt{2}D_{(\epsilon l_B)^2/2}(\sqrt{2}p_y l_B) = 0, \quad (9)$$

which follows from the condition of continuity of the wave function at the edge of the step, where $D_p(x)$ are the parabolic cylinder functions [10]. The resulting dispersion relations are illustrated in Fig. (2). We see that edge states emerge at threshold values of the negative longitudinal momentum, and for increasing $|p_y|$ they rapidly approach the (relativistic) bulk Landau levels.

3 Magnetic dot

The perfect reflection of low-energy graphene's quasiparticles on a magnetic barrier discussed in the previous section suggests that it is possible to create *magnetic quantum dots*, where the quasiparticles are confined by an appropriate magnetic field configuration. We shall now focus on a cylindrically symmetric dot, defined by a radially inhomogeneous field $\mathbf{B} = B(r)\hat{e}_z$. It is then

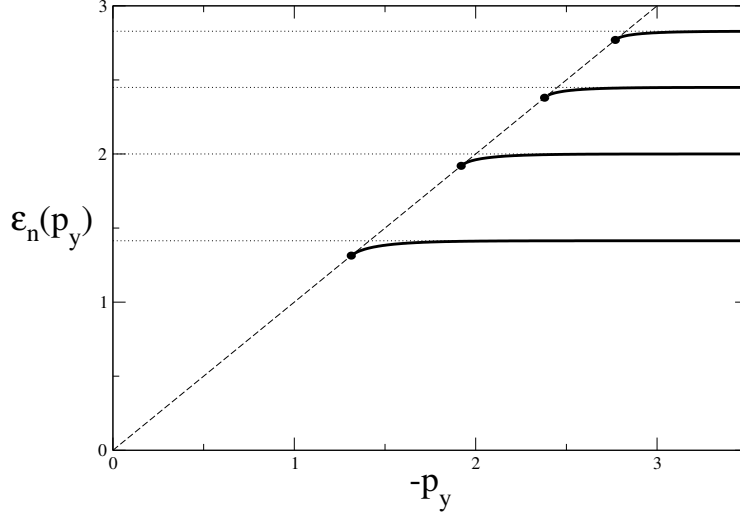


Fig. 2. Spectrum of the lowest-energy edge states. The momentum is expressed in units of l_B^{-1} and the energy in units of v_F/l_B . The dotted lines correspond to the relativistic bulk Landau levels $\sqrt{2n}$, with n positive integer.

convenient to express the vector potential as

$$(A_x, A_y) = c(-y, x)\varphi(r)/er^2, \quad (10)$$

where $\varphi(r)$ is the magnetic flux through a disc of radius r in units of the flux quantum hc/e ,

$$\varphi(r) = \frac{e}{c} \int_0^r dr' r' B(r'). \quad (11)$$

To solve the Dirac-Weyl Hamiltonian (1) with the vector potential (10), we note that it commutes with the operator $J = L + \sigma_z/2$, where $L = x\partial_y - y\partial_x$ is the z -component of the orbital angular momentum. As a consequence, we can choose its eigenstates in the form

$$\begin{pmatrix} \psi_+ \\ \psi_- \end{pmatrix} = \frac{1}{\sqrt{2\pi}} \begin{pmatrix} \phi_m(r) e^{im\vartheta} \\ \chi_m(r) e^{i(m+1)\vartheta} \end{pmatrix}, \quad (12)$$

where $x + iy = re^{i\vartheta}$ and m is an integer. Using the ansatz (12), Dirac equation (1) reduces to a pair of coupled 1D equations for the radial part of the spinor components $\phi_m(r)$ and $\chi_m(r)$ (where $r \geq 0$ and $f' = df/dr$),

$$\phi_m' - \frac{m + \varphi(r)}{r} \phi_m = i\epsilon\chi_m, \quad (13)$$

$$\chi'_m + \frac{m+1+\varphi(r)}{r}\chi_m = i\epsilon\phi_m.$$

which result in a second-order equation for $\phi_m(r)$,

$$\phi_m'' + \frac{1}{r}\phi_m' + \left(\epsilon^2 - \frac{e}{c}B(r) - \frac{(m+\varphi(r))^2}{r^2} \right) \phi_m = 0. \quad (14)$$

χ_m then directly follows from ϕ_m via Eq. (13), except in the case of zero-energy, where one has to solve directly the first order decoupled equations. Equation (14) can now be studied for different magnetic field profiles. We shall consider here a simple model for a magnetic dot, whereby the field vanishes inside a disk of radius R and is given by $B = B_0$ outside. We shall see that this profile leads to discrete energy levels, similarly to the case of a conventional quantum dot with electrostatic confinement in a 2DEG. The flux $\varphi(r)$ reads

$$\varphi(r) = \frac{r^2 - R^2 r}{2l_B^2} \theta(r - R), \quad (15)$$

where the magnetic length defined outside the dot is given by $l_B = \sqrt{c/eB_0}$.

The solution of Eq. (13) for zero energy is straightforward. The eigenfunctions are

$$\psi_m^{\epsilon=0} = \mathcal{N}_m \left(\frac{r}{R} \right)^{\theta(r-R)R^2/2l_B^2} e^{-\varphi(r)/2} \begin{pmatrix} 0 \\ \frac{e^{-im\theta}}{r^m} \end{pmatrix},$$

where \mathcal{N}_m is a normalization constant and $m \leq 0$. It is interesting that only the down (iso)-spin component is non-vanishing, implying that for these states the amplitude of the wave function on one of the graphene's honeycomb sublattices vanishes. The non-zero energy eigenvalues come in pairs $\pm\epsilon$, and we focus on the $\epsilon > 0$ sector. The general solution of Eq. (14) consists of a Bessel function inside the dot, $\phi_m^< = J_m(\epsilon r)$ for $r < R$, and a combination of degenerate hypergeometric functions Φ and Ψ [10] in the external region $r > R$:

$$\phi_m^> = \xi^{|\tilde{m}|/2} e^{-\xi/2} (a_1 \Phi(\alpha, 1 + |\tilde{m}|; \xi) + a_2 \Psi(\alpha, 1 + |\tilde{m}|; \xi)). \quad (16)$$

where $\xi = r^2/2l_B^2$, $\tilde{m} = m - \delta$, and $\delta = R^2/2l_B^2$ is the missing flux through the dot in units of the flux quantum. Here $a_{1,2}$ are arbitrary complex coefficients, and energy is parameterized as

$$(\epsilon l_B)^2/2 = 1 + \tilde{m}\theta(\tilde{m}) - \alpha. \quad (17)$$

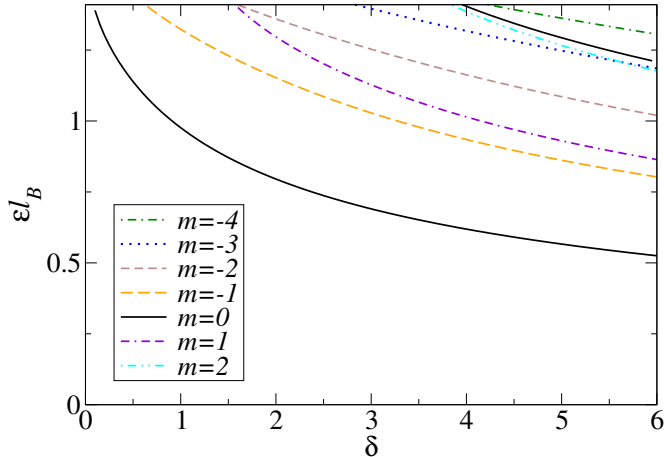


Fig. 3. (Color online) Low-energy eigenenergies (labeled by m) for a disk-like magnetic quantum dot in graphene versus missing flux $\delta = R^2/2l_B^2$.

Continuity of the wave function at $r = R$ now implies continuity of both $\phi_m(r)$ and $\phi'_m(r)$, see Eq. (13), and the resulting two matching conditions determine the energy spectrum. In the limit $R = 0$ Eq. (14) reproduces the well-known relativistic Landau levels, corresponding to $\alpha = -n$, with $n = 0, 1, 2, \dots$ [8], where Φ and Ψ reduce to Laguerre polynomials. For finite R , one can show that the matching problem does *not* admit solutions with $\alpha = -n$ [7], and normalizability of the wave function for $\alpha \neq -n$ requires $a_1 = 0$ in Eq. (16). Then one of the two matching conditions fixes a_2 , and the other leads to the quantization condition which determines the energy levels in graphene's magnetic dot:

$$1 - |\tilde{m}|\theta(-\tilde{m})/\delta - \frac{\epsilon l_B}{\sqrt{2\delta}} \frac{J_{m+1}(\epsilon l_B \sqrt{2\delta})}{J_m(\epsilon l_B \sqrt{2\delta})} = \frac{d}{d\xi} \ln \Psi(\alpha, 1 + |\tilde{m}|; \xi = \delta). \quad (18)$$

Eq. (18) can be solved numerically, and the lowest positive energy levels are illustrated in Fig. 2 of [7]. We notice that, whereas the bulk Landau states are highly In Figure 3, we show the solutions to Eq. (18) with $\epsilon > 0$ but below the lowest positive-energy bulk Landau level located at $\epsilon l_B = \sqrt{2}$. Within the shown δ range, for $m \neq 0$, there is at most one solution with $0 < \epsilon l_B < \sqrt{2}$, while for $m = 0$, we obtain two such solutions for $\delta \gtrsim 4$. Depending on the missing flux $\delta \sim R^2 B_0$, the energy levels of this 'Dirac dot' can be tuned almost at will.

To conclude, we have discussed the properties of graphene's Dirac quasiparticles in two different inhomogeneous magnetic field profiles. In particular we described a new way of confining Dirac-Weyl quasiparticles by means of magnetic barriers. We hope that our work will guide experimental efforts to the development of mesoscopic structures based on this novel material, and stimulate more theoretical work on the effects of magnetic barriers on Dirac

fermions.

We thank A. Altland, T. Heinzl, and W. Häusler for discussions. This work was supported by the SFB TR 12 of the DFG and by the ESF network INSTANS.

References

- [1] K.S. Novoselov *et al.*, Science **306**, 666 (2004); Nature **438**, 197 (2005).
- [2] Y. Zhang, Y.W. Tan, H. Stormer, and P. Kim, Nature **438**, 201 (2005).
- [3] C. Berger *et al.*, Science **312**, 1191 (2006).
- [4] S.Y. Zhou *et al.*, Nature Physics **2**, 595 (2006).
- [5] For a pedagogical review, see A. Calogeracos and N. Dombey, Contemporary Physics **40**, 313 (1999).
- [6] M.I. Katsnelson, K.S. Novoselov, and A.K. Geim, Nature Physics **2**, 620 (2006).
- [7] A. De Martino, L. Dell'Anna, and R. Egger, preprint cond-mat/0610290.
- [8] G.W. Semenoff, Phys. Rev. Lett. **53**, 2449 (1984).
- [9] D.P. DiVincenzo and E.J. Mele, Phys. Rev. B **29**, 1685 (1984).
- [10] I.S. Gradshteyn and I.M. Ryzhik, *Table of Integrals, Series, and Product* (Academic Press, Inc., 1980).